Materials & Design 265 (2026) 115866

Contents lists available at ScienceDirect

Materials & Design

journal homepage: www.elsevier.com/locate/matdes

Bio-based poly(furfuryl alcohol) resin as a sustainable matrix alternative for prepregs

Dennis Budelmann *, Bodo Fiedler

Institute of Polymers and Composites (IPC), Hamburg University of Technology, Denickestr. 15, D-21073 Hamburg, Germany

ARTICLE INFO

Keywords:
Materials engineering
Composites
Fiber reinforced plastics
Polymers
Renewable feedstock
Processing

ABSTRACT

Despite their ecological superiority and competitive thermo-mechanical performance compared to petrochemical matrices, furan resins based on poly(furfuryl alcohol) (PFA) have so far played a minor role in composite applications. This is due to a demanding manufacturing process, which involves long curing cycles and specialized equipment for removing water from polycondensation to produce low-porosity parts. This work employs resin pre-curing (B-staging) to tailor PFA bio-resin properties for prepreg applications, while reducing the porosity in a fully cured state. A PFA prepolymer with a bio-content of 98 wt% was synthesized before heat treatments were applied for B-staging and final curing of the acid-catalyzed prepreg resin. The influences on viscosity, resin reactivity and chemistry, molecular weight, volatile separation, density, and porosity were investigated. It was found that an isothermal 120-minute B-staging procedure at 60 °C resulted in rheological behavior matching the processing properties of commercial, aerospace-grade epoxy prepregs. It was demonstrated that B-staging reduces volatile separation and associated void formation in the final curing step. Fully cured PFA samples with a porosity of less than 3 % could be produced employing short curing cycles. The findings advance the understanding of sustainable lightweight materials by tailoring PFA resins as potential polymer matrices for bio-prepregs.

1. Introduction

Sustainability concerns and increasing regulatory pressure put on industries, along with a declining supply security of petrochemical-based precursors, have substantially raised the interest of bio-based thermoset resins for advanced composite manufacturing [1,2]. Comprehensive life cycle assessments (LCA) demonstrated that composite materials made from renewable feedstock can reduce the carbon footprint of individual applications in various industries such as aviation [3], automotive [4] and marine [5]. The ecological benefits, however, are heavily affected and may even be nullified by aspects related to inferior and fluctuating properties, required energy consumption, and land use [6]. With respect to the latter, dedicated land cultivation may be critical due to an inevitable competition with land use for food production [7]. A potential solution to this dilemma is to utilize agricultural waste from food production to source biomass for green chemicals.

One relevant representative of this approach is furfural, a platform compound which is produced from lignocellulosic biomass, e.g., sugarcane bagasse, rice husk or corn cobs, and can be synthesized into furfuryl alcohol (FA) by hydrogenation [8]. Driven by pioneer work on furanchemistry conducted by Dunlop and Peters in mid-20th century [9], FA was found to be able to self-polymerize into a dark viscous liquid (furan resin) and to eventually form a solid thermoset polymer network upon final cure. The condensation reaction to polyfurfuryl alcohol (PFA) is promoted by heat, acidic catalysts, alumina, and others [10] and has been studied extensively as recently reviewed by Iroegbu and Ray [11]. The authors emphasize that despite the high research effort, the complex resinification process including linear chain growth by dehydration, color changes by abstraction of hydride ions and network formation by Diehls-Alder reaction is yet to be fully understood.

Today, PFA resins are mainly used in foundry as binders for sand casting [12] and, with less industrial relevance, for wood preservation [13] and improved chemical resistance of concrete [14]. For load-bearing composite applications, the most utilized commercially available PFA in academic research is most likely the Furolite® resin by Transfuran Chemicals, Belgium which has been used in several studies on cure kinetics and chemistry [15–18] as well as composite manufacturing and performance [19,20]. Meanwhile, a handful of

* Corresponding author.
E-mail address: dennis.budelmann@tuhh.de (D. Budelmann).

https://doi.org/10.1016/j.matdes.2026.115866
Received 5 January 2026; Received in revised form 24 February 2026; Accepted 17 March 2026
Available online 18 March 2026

commercial PFA-based prepreg systems is available from material suppliers including Mitsubishi Chemicals, Simcas Composites, and SHD Composites. These prepregs are delivered in a pre-cured state (B-stage) which serves the purpose of adjusting processing properties such as tack and drape as well as reducing resin bleed during cure, respectively [21]. However, despite their competitive thermo-mechanical properties [22] and excellent fire, smoke, toxicity (FST) characteristics [23], which make PFA resins a potential substitute for phenolics, a widespread use in the composites industry is still pending.

The main technological challenges hindering the widespread industrial use of PFA resins in composite materials are related to the aforementioned polycondensation reaction. During the linear chain growth condensation reaction, a total of up to 1 mol water per 1 mol FA is produced in theory [24] equaling 18.4 wt% of chemical water to be discharged. The water will evaporate at high cure temperatures leading to massive void formation and porosity which reduces the mechanical part performance. For their comprehensive review article on PFA composites, Odiyi et al. [25] concluded that long step-wise curing cycles of up to 96 h are often applied to suppress void formation to the detriment of economic efficiency. The lengthy manufacturing process cycles have been a significant drawback that has limited the industrial scaling. Other porosity mitigation strategies were proposed, e.g., repeated ventilation in molding processes or double vacuum bag technology [26]. However, these techniques require either additional process steps or more sophisticated manufacturing equipment making PFA composites less attractive for cost-sensitive applications. In an effort to overcome the porosity issue, Resch-Fauster et al. [27] investigated the potential of natural fibers to absorb water produced upon curing a commercial PFA resin. A significant porosity reduction within the manufactured composites was achieved when using highly hydrophobic fibers even for short and high-temperature curing cycles. To the best of the authors' knowledge, no research has yet been conducted that addresses the porosity issue of PFA resins specifically tailored for prepregs.

Therefore, the objective of the present study is to investigate cure-related water separation and void formation of PFA resins with a view to their utilization as prepreg matrices for advanced composite manufacturing. It is hypothesized that purposive pre-curing (B-staging) of the matrix component can reduce the release of water and other volatiles to such an extent that components with reduced porosity can be produced within short cure cycles. Therefore, a FA-based prepolymer is synthesized and pre-cured into different B-stages by applying isothermal temperature profiles. Changes in rheology are monitored to obtain insights into the resin processing properties. Water release and cure kinetics are studied employing thermogravimetric analysis (TGA) and differential scanning calorimetry (DSC). The combination of methods enables simultaneous tracking water evaporation and PFA cure progression as well as considering the volatile weight loss. Finally, the success of part quality improvement through B-staging is evaluated by investigating the porosity of cured PFA samples via microscopy. Despite aiming for prepreg applications in the long run, all experiments of the study are carried out on neat resin without reinforcement fibers. It is reasoned that for porosity investigation, absence of fibers helps to set aside the effects of mechanical entrapment, interface between resin and fibers, and chemical agents that may be present on the fibers [28].

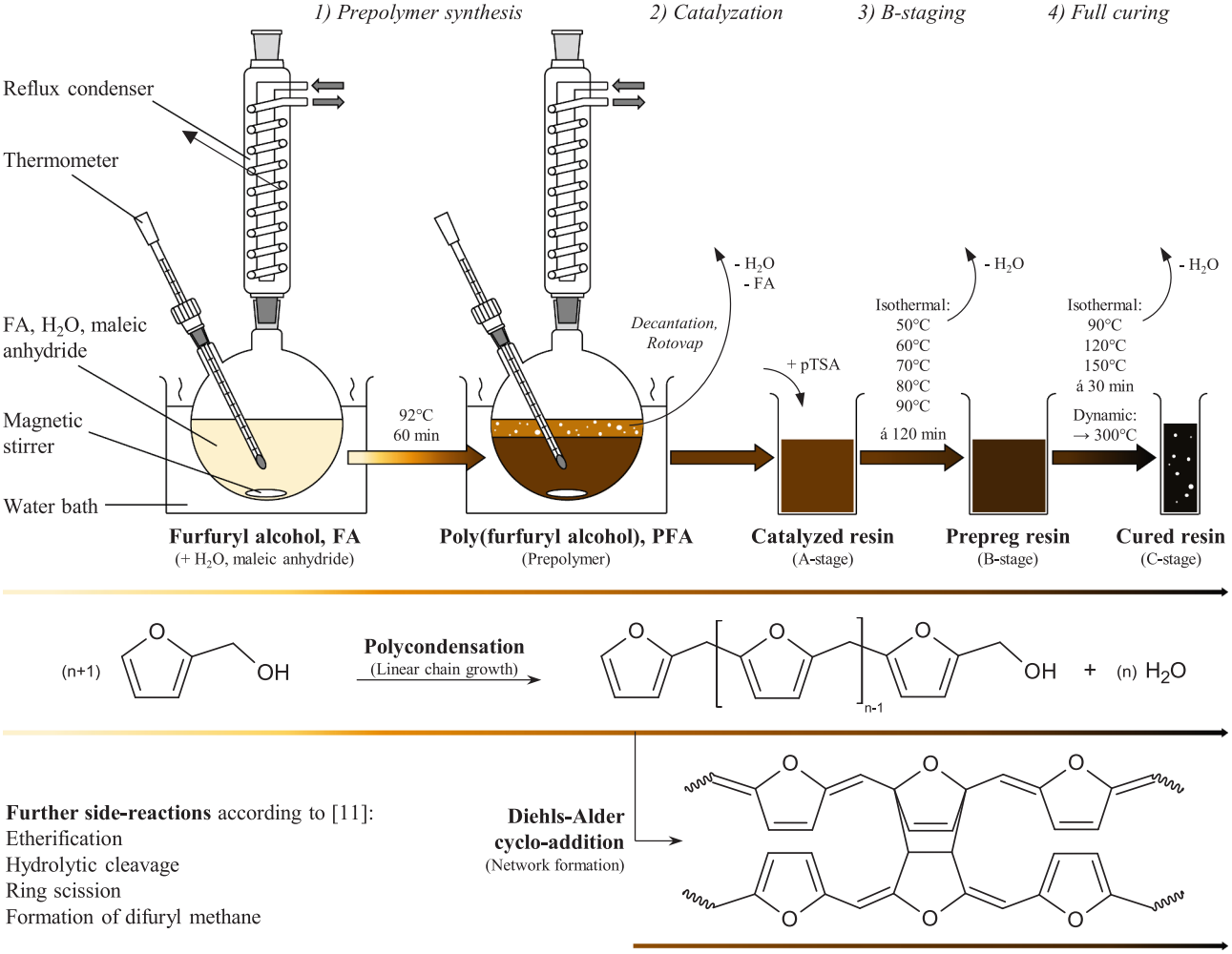

Fig. 1. Synthesis, processing route and main reaction schemes of poly(furfuryl alcohol)-based prepreg resin.

2. Materials

For furan resin synthesis, furfuryl alcohol (FA, 98.5 %, 98.10 g mol^{-1}), maleic anhydride (MA, 99 %, 98.06 g mol^{-1}), p-toluenesulfonic acid monohydrate (pTSA, 98.5 %, 190.22 g mol^{-1}) and deionized water, 18.02 g mol^{-1}) were purchased from Merck, Germany. All chemicals were used as received. The steps, which were involved in the resin preparation process and are described in the following sections 2.1 to section 2.3, can be followed according to Fig. 1.

2.1. Polyfurfuryl alcohol (PFA) prepolymer synthesis

In a first step, a prepolymer based on polymerized furfuryl alcohol (polyfurfuryl alcohol, PFA) was synthesized according to the procedure described by Wewerka et al. [29]. Therefore, 0.26 g of MA were dissolved in 53.4 g of deionized water and added to 150 g of FA in a 250 ml two-neck flask. The solution was refluxed at 92 °C for 60 min under rigorous stirring to advance the polymerization reaction. The initially light-yellow liquid turned into the furan resin-specific dark brown color within the first 10 min of synthesis. Shortly after, the solubility limit was reached indicated by a phase separation between the dark resin and a top layer of water and unreacted FA. From this point on, the resin viscosity visibly increased as a function of reaction time. After 60 min of prepolymerization, the synthesis product was cooled down before decanting the top layer of water and unreacted FA. Remaining low molecular weight fractions were removed by rotatory evaporation at 50 °C for 60 min. The prepolymer at this stage had a PH of 1.9. Opposing to Wewerka's original procedure, the resin was not PH-neutralized by adding sodium hydroxide as no further increase in viscosity was measured via rheometry even after two weeks of ambient exposure. Despite showing minimal reactivity at room temperature, the prepolymer was stored at −18 °C until further processing.

2.2. Catalyzed resin (A-stage)

In order to prepare the final reactive one-pot resin that can be used for prepreg production, the prepolymer was defrosted and heated to room temperature. 2 wt% of pTSA were used as a catalyst and added to the prepolymer in form of a 25 % solution in deionized water under mechanical stirring. The amount of acid catalyst was determined based on preliminary tests on the observed resin reactivity. The catalyzed resin was degassed for 5 min at room temperature before further usage and will be referred to as 'A-stage' resin in the following.

2.3. Pre-cured (B-stage) and fully cured (C-stage) prepreg resins

Pre-curing (B-staging) and full curing (C-staging) were performed on the catalyzed A-stage resin of section 2.2 by applying consecutive heat treatments as shown in Fig. 2. For B-staging, five alternative isothermal temperature steps between 50 and 90 °C were employed in order to create different pre-curing states while the dwell time was kept constant at 120 min. For subsequent full curing, three 30-minute isothermal steps were set at 90, 120 and 150 °C (Fig. 2, isothermal cycle). In an effort to isolate the impact of B-staging, direct curing cycles from A to C-stage were applied as reference measurements in absence of a preceding B-staging. Additional dynamic temperature sweeps from room temperature to 300 °C at 5 K min^{-1} were carried out to set a benchmark for a maximum high-temperature curing state (Fig. 2, dynamic cycle). All heating and cooling ramps between isothermal dwells were run at 5 K min^{-1}.

3. Methods

3.1. Rheology

Viscoelastic characterization of neat PFA prepolymer and pTSA-catalyzed resin was performed as oscillatory rheometry (Malvern Kinexus Ultra+). A constant normal force of 0 N was chosen over a constant gap due to curing-related water evaporation and shrinkage during measurement while running a plate-plate configuration of 40 mm diameter. The complex viscosity η*, viscoelastic storage modulus G' and loss modulus G" as well as the corresponding loss factor tan δ were measured. Temperature and isothermal time sweeps were carried out in accordance with the curing cycles presented in section 2.3. For isothermal dwell, the gel times of catalyzed resin were determined at the crossover point of G' and G" equaling a tan δ of 1.

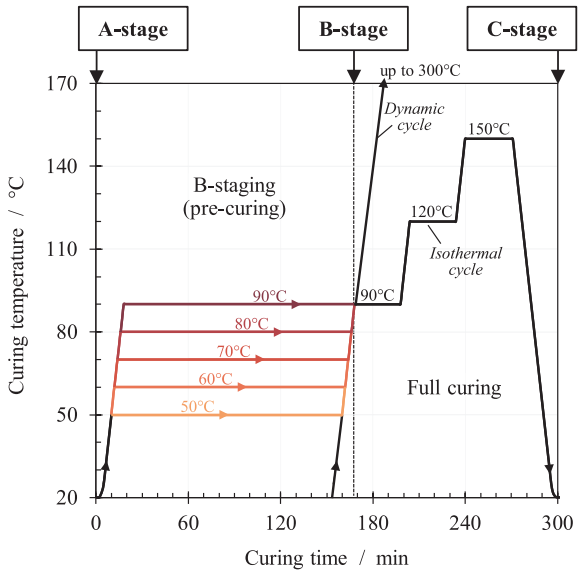

Fig. 2. B-staging and curing cycles for pTSA-catalyzed PFA resins.

3.2. Thermogravimetric analysis (TGA)

TGA (TA Instruments Q500) was applied to monitor the relative amount of evaporated water which is produced as a byproduct of polycondensation and can be used as a measure of cure progression for linear chain growth. In an effort to create equal cure conditions as for DSC, 10 ± 0.5 mg of pTSA-catalyzed prepolymer were transferred to aluminum DSC crucibles with a pierced lid. In addition to the basic weight loss information, derivative thermography (DTG) graphs were constructed which show the rate of mass change pinpointing the temperature of maximum conversion. Mass loss by TGA was monitored while applying the B-staging and curing cycles outlined in section 2.3. Purge flows were set at 60 ml of synthetic air during heating and 60 ml of N_2 for cooling.

3.3. Differential scanning calorimetry (DSC)

Modulated DSC (Netzsch DSC 204 F1 *Phoenix*) was used to monitor the cure progression of the pTSA-catalyzed PFA prepolymer. In addition to the aforementioned cure cycles, dynamic temperature profiles of 1, 2, 5 and 10 K min^{-1} between −50 and 300 °C were run. The modulation period was set at 60 s while the amplitude was adjusted to the heating rates in such a way that cooling (heat-iso) was excluded. The degree of (pre)cure (DoC) from B-staging was calculated as the enthalpy ratio between both B-staged and fresh resin.

10 ± 0.5 g of PFA were analyzed in aluminum pans with pierced lids to enable water evaporation analogous to TGA. Other than standard DSC analysis of phenolics utilizing sealed high-pressure crucibles, evaporation was permitted in this study to emulate the curing process during composite manufacturing. As the water from polycondensation is continuously split off, the weight of the sample is reduced leading to

falsified specific enthalpies. Therefore, the time- and temperature-dependent enthalpies are adjusted by using the corresponding mass data from TGA.

3.4. Gel permeation chromatography (GPC)

GPC (Malvern Viscotek GPCmax VE2001) was performed to examine the evolution of the molecular weight of the PFA resins throughout B-staging. Resin samples were pre-cured at 60 °C for 0, 15, 30, 60 and 120 min, then were dissolved in tetrahydrofuran (THF). The sample cured for 120 min did not fully dissolve in THF so that only the dissolved part was analyzed. Three columns connected in series were used including a pre-column TGuard Organic Guard Column (10•4.6 mm) and two mixed bed separation columns LT3000L (300•8 mm). Elution was monitored with a Malvern Viscotek TDA 305 refractive index (RI)- and viscosity detector. The flow rate was set to 1 ml min^{-1} and 100 µl were injected at a temperature of 35 °C.

3.5. Fourier Transform infrared spectroscopy (FTIR)

FTIR (Bruker Tensor II) spectra of A- and B-stage resins were acquired in attenuated total reflectance (ATR) using the MIRacle™ Single Reflection Horizonal ATR accessory (PIKE Technologies). The measurements were conducted at a spectral resolution of 2 cm^{-1}. Four sample spectra were averaged in the mid-infrared (MIR) range from 4000 to 400 cm^{-1} and cut at 630 cm^{-1}. Prior to each experimental run, 40 background spectra were recorded from the ambient atmosphere within the sample chamber. The processing of raw data included baseline correction using the concave rubberband method with five iterations. Normalization was performed on the furan ring C=C stretching peak at 1505 cm^{-1} which is considered chemically invariant during the B-staging process due to its high stability across different polymerization stages.

3.6. Porosity determination of cured PFA resin samples

In order to quantify porosity induced by water release upon cure, catalyzed PFA was cured in test tubes and analyzed by light microscopy following the procedure shown in Fig. 3. Therefore, both A-stage resins catalyzed by pTSA and B-stage resins were thoroughly stirred and transferred to test tubes with a sample size of 4 g. The resins were subjected to the temperature profiles in a programmable oven at atmospheric pressure. After cure, the glass test tubes were carefully smashed before grinding the cured resin columns to gain flat coin-like specimens.

The porous surfaces were analyzed by light microscopy using a Keyence VHX-6000 in combination with a Keyence VH-Z100R universal zoom lens (100x to 1000x). Images were taken at 100x, stitched and converted to 8-bit greyscale before defining a threshold to highlight and measure porosity. The area occupied by pores was set in relation to the total surface area giving a porosity value Φ. The procedure was repeated for every sample at three different depths (Fig. 3, left) to calculate a mean value representative of the cured sample. Furthermore, the density was determined via Archimedes' principle by using water as the immersion fluid and a density determination kit attached to a Mettler Toledo AT261 microscale.

4. Results

4.1. A-stage PFA resin

The rheological behavior determines the PFA resin's processing and prepregging properties and will be examined in the following. It also provides information on the success of B-staging when being compared to commercial prepregs. The complex viscosities of PFA prepolymer and pTSA-catalyzed resin are plotted as a function of temperature in Fig. 4. The initial room temperature viscosity of synthesized PFA prepolymer was 2.5 Pa s which fell into the same range as the ~ 7 Pa s reported by [17] for a commercial PFA resin. In contrast, it was significantly lower than 150 Pa s measured in another study [30] after following the same PFA synthesis route. The increased viscosity may have originated from higher temperatures and longer dwell times in the rotational evaporator. In the further course of the prepolymer graph (Fig. 4), 50 mPa s were reached at 90 °C without indication of an onset of cross-linking.

The catalyzed PFA resin in A-stage showed similar rheological behavior in the low-temperature regime. However, the curve had a slightly more erratic trajectory, which was most likely due to phase separation of the water-containing acid catalyst. Within the mid-temperature range, curing-related solidification began to exceed the temperature-induced viscosity reduction eventually leading to formation of a gel. The minimum viscosity of the A-stage resin was found to be close to 100 mPa s at 60 °C for the investigated rate ramp of 5 K min^{-1}. Meanwhile, the viscosity of the prepolymer steadily decreased to 60 mPas, approaching the lower temperature-dependent limit. At this stage, the catalyzed resin viscosity appeared to be low enough to achieve

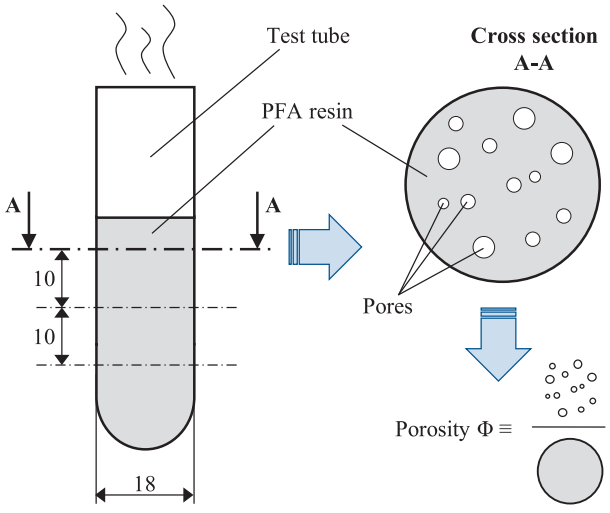

Fig. 3. Sample preparation for the determination of cured resin porosity by microscopy. Illustration not to scale.

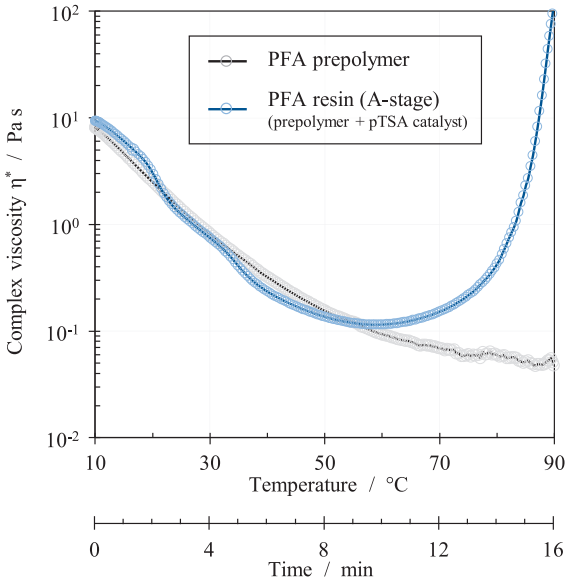

Fig. 4. Viscosities of PFA prepolymer and catalyzed PFA resin (A-stage) subjected to 5 K min^{-1} temperature sweeps.

adequate impregnation during resin infusion and prepregging processes, respectively.

Since the curve indicated an onset of cure in this temperature range, processing may be compromised by the risk of pre-mature gelation. As a consequence, the temperature-dependent gel times t_{gel} were assessed by applying isothermal cure profiles in form the G'-G" crossover as shown in Fig. 5. As expected, the gel times decreased rapidly as a function of cure temperature. For cure temperatures of 70 °C and beyond, a limit value of about 15 min was reached. Note that the gel times included a heating period from room temperature at 5 K min^{-1} which took at least 10 min to reach target temperatures of > 70 °C. Hence, the gel times in this instance did not approach zero for very high temperatures. Based on the findings, a prepregging temperature around 50 °C to produce PFA prepregs is recommended. At this temperature level, the viscosity of ~ 100 mPa s will facilitate void-free impregnation while maintaining a conveniently long processing window of more than two hours.

4.2. B-staging (pre-curing)

B-staging of prepregs is commonly performed to increase resin viscosity giving the prepreg favorable processing characteristics including tack and drape, while reducing resin bleed. As desirable viscosity levels for prepregs are well-known for established prepreg systems based on epoxy, the aim was to replicate those viscosities for PFA resins. In an effort to identify heat treatments leading there, isothermal temperature profiles were applied on A-stage resins for 120 min – the same as used for the determination of gel times (Fig. 5).

4.2.1. Rheological effects of pre-curing

Fig. 6 shows the progression of viscosity for isothermal B-staging between 50 and 90 °C. After the heating-related viscosity drop, the viscosities increased as a result of cure progression. The graphs were indicative of temperature-specific viscosity limits which both increased and were approached quicker for higher temperatures. For all dwells, the limit values, however, were not reached within the tested 120 min yet. Instead, the viscosities of the B-staged resins ranged between 10^2 Pa s (50 °C) and $5•10^4$ Pa s (90 °C) at the corresponding temperatures. High temperature B-staging at 80 °C and especially 90 °C was linked to fluctuation in the graph which may be the result of volatile bubbles that were hindered to dissipate at high viscosities.

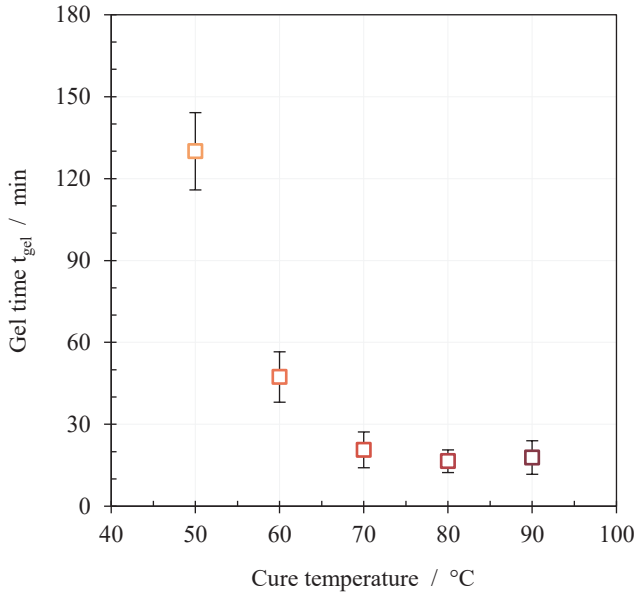

Fig. 5. Gel times of catalyzed PFA resins (A-stage). The displayed gel times include the durations of heating from room temperature to target temperature at 5 K min^{-1}.

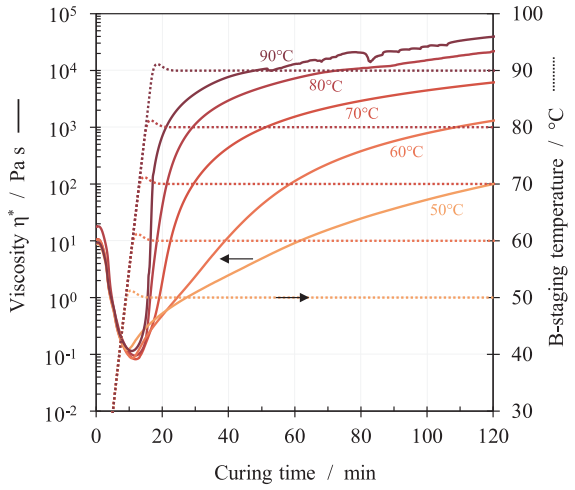

Fig. 6. Viscosity evolution of PFA resin during isothermal B-staging.

Additional temperature sweeps, which were performed by cooling at 5 K min^{-1} immediately after B-staging, yielded the rheological data presented in Fig. 7. The sweeps represented the processing-relevant temperature range, e.g., for automated prepreg lay-up processes such as AFP, between room temperature and the respective B-staging temperatures. The PFA resins pre-cured at 70, 80 and 90 °C reached high room temperature viscosities of up to $1.5•10^5$ Pa s. Surprisingly, independence of viscosity from temperature was observed here for lower temperatures. The storage moduli G' plotted on the right-hand side of the graph followed the same trends. While B-staging at 50 °C led to relatively low viscosities, the rheological data of PFA resin pre-cured at 60 °C very accurately replicated the data of an aero-space grade, epoxy-based prepreg resin (Hexcel's 8552, black lines) that was characterized previously [31]. A viscosity of 10^4 Pa s and a corresponding G' of 10^5 Pa were found at temperatures between 35 and 40 °C – a temperature range which has repeatedly been demonstrated to result in a favorable maximum of tackiness for both epoxy [32,33] and phenolic prepregs [34]. Furthermore, the Dahlquist criterion (G' < $3•10^5$ Pa) was satisfied which is prerequisite for tack of pressure sensitive applications and has been proven to be applicable to prepregs in a similar manner. With a view to drapability at room temperature, the B-staged resin films did not

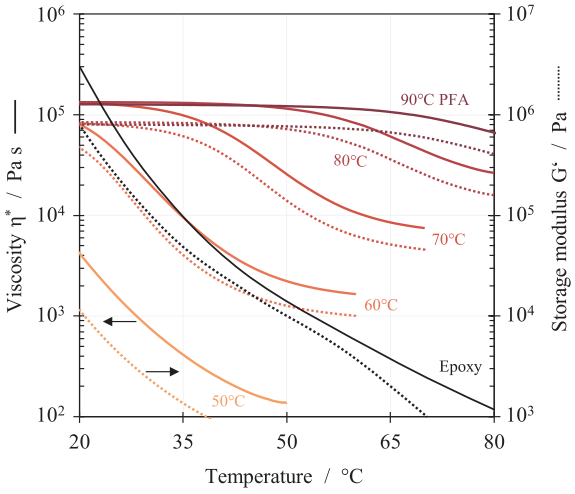

Fig. 7. Temperature-dependent viscosity and storage modulus of pTSA-catalyzed PFA prepreg resin after 2 h of B-staging at 50, 60, 70, 80 and 90 °C. Rheological data of a commercial epoxy prepreg resin [31] was added in black.

flow but subjectively appeared flexible enough for further processing. From this perspective, pre-curing the investigated PFA prepreg resin at 60 °C has the potential to yield advantageous processing characteristics such as tack and drape which will be investigated in future research endeavors.

Comparing the rheological results to data sheets provided by material manufacturers for commercial PFA prepregs revealed that the resins studied here were generally more viscous. Two commercial prepregs, i.e., Mitsubishi's CP103 and Simcas composite's PFC502 were specified with a rather low viscosity of 5 Pa s at 50 °C. However, no information was given as to whether this value applies to A-stage or B-stage prepreg resin. The low value suggested the latter. SHD composite's PFA prepregs FR30 (300 Pa s) and PS200 (200 Pa s), however, ranged between resins that were B-staged at 50 °C and 60 °C for 120 min.

4.2.2. Volatiles separation

In addition to tailoring processing properties, it was hypothesized that B-staging also reduces void formation upon final curing, since a significant amount of water by-product from polycondensation has already been produced and discharged during pre-curing. Therefore, the portion of volatiles split off during B-staging and final cure was monitored by TGA.

Fig. 8 displays the relative weight loss and loss rates that is the derivative of weight loss over time (isothermal A-stage to B-stage and dynamic B-stage to C-stage) as well as the derivative of weight loss over temperature (dynamic B-stage to C-stage). Table 1 provides the most important corresponding data that can be read from the graphs. The loss rates of all B-staging procedures shown in the left graphs started to increase rapidly during heating before reaching the maxima as soon as the target temperatures had been adjusted. Especially in the low temperature regime, the weight loss was attributed to evaporating water that had either been present in the resin initially or was formed as the byproduct of polycondensation. The maximum rate decreased as a function of temperature from 0.581 ± 0.099 wt% min^{-1} at 70 °C to 0.309 ± 0.065 wt% min^{-1} at 50 °C. Variations between the high temperature levels involved no significant influence on the loss rate. It was still found that the weight loss after 120 min of pre-curing steadily increased for higher temperatures as shown in Fig. 9a. The range covered mass losses between 8.18 ± 0.35 wt% for 50 °C and 12.94 ± 1.34 wt% which resulted in an average increase in weight loss of 1.2 wt % per 10 °C pre-curing temperature. Analogous to the observations made during the rheological analysis in section 4.2.1, irregularities in the high temperature curves were present. This was due to bubbles that formed as water from polycondensation could not dissipate quick enough through diffusion and evaporation.

If the B-staged resins were subsequently exposed to dynamic temperature profiles, the weight loss curves converged in a narrow corridor of 17.16 ± 1.15 % weight loss as displayed in the right graph of Fig. 8. Only a minimal linear upwards trend in the final volatile loss was found when plotting the data as a function of B-staging temperature (Fig. 9b). This finding implicates that the B-staging procedure had significant influence on the intermediate prepreg resin properties but a similar state was eventually be reached after C-staging as far as the volatile weight loss was concerned. The loss rate did not fully return to zero towards the end of the cure cycle which indicated further diffusion of volatiles out of the cured resin at higher temperatures. At this stage, the TGA curve might also have been influenced by an overlap of initiated decomposition. Guigo et al. studied the thermal degradation behavior of cured, MA-catalyzed PFA resins and found the onset to be between 250 and 300 °C and the decomposition temperature (initial 10 % of weight loss) to be 340 °C [35].

As stated before, the maximum loss rates during B-staging increased as a function of temperature up to 70 °C before becoming independent from temperature (Fig. 9c). During full curing (Fig. 9d), however, the opposite trend could be observed: The higher the B-staging temperature, the fewer unreacted species were available for the chain growth and cross-linking reaction during C-staging. As a consequence, less water-byproduct was produced upon final cure which may result in lower resin porosity and higher part quality. This hypothesis will be explored in detail in section 4.3.2 by examining the cure-related void formation in neat PFA resin. Furthermore, it was mainly indicative of the linear chain growth and did not uncover crosslinking because no volatiles were split off during the Diehls-Alder reaction which was reported to be responsible for PFA network formation [36]. Therefore, additional DSC measurements were conducted using the same temperature profiles and identical sample preparation.

4.2.3. Pre-curing monitored via DSC, GPC and FTIR

Table 2 displays the final cure enthalpies released by fresh and B-staged PFA resins throughout a 5 K min^{-1} temperature ramp to 300 °C. Fresh PFA released 130 J g^{-1} which was lower than the 165–222 J g^{-1} (depending on heating rate) reported by [16] for the commercial Furolite® PFA resin, cured with a comparable amount of pTSA. Analogously, the authors reported a lower peak reactivity temperature of ~ 90 °C compared to this study's 102 °C indicating higher reactivity. The discrepancy most likely originated from differences in the level of

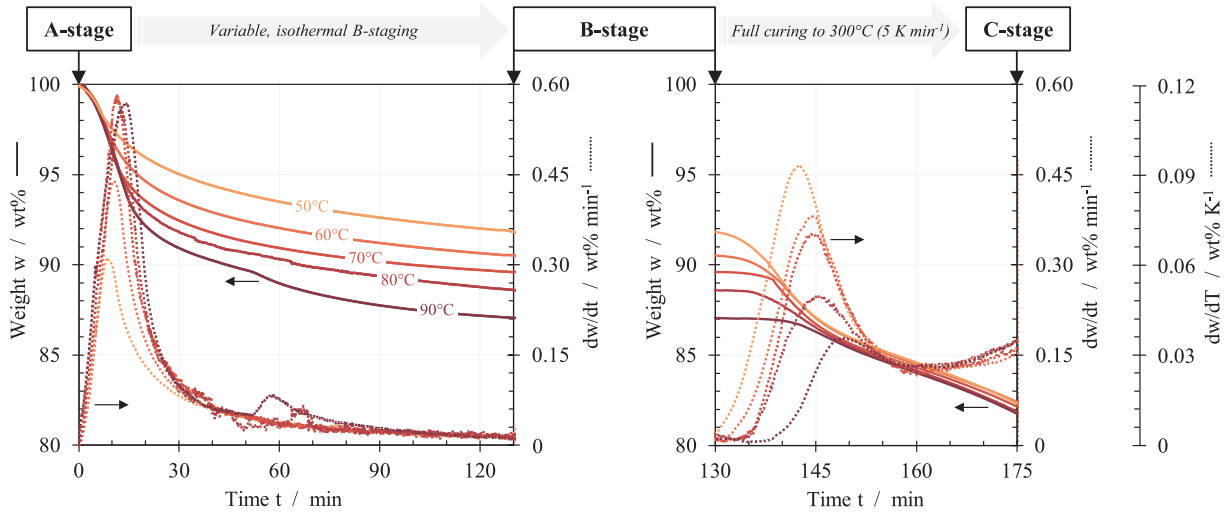

Fig. 8. TGA results of catalyzed PFA resin: volatile weight loss and corresponding loss rates for isothermal B-staging procedures carried out at different temperatures (50, 60, 70, 80 and 90 °C, left) and subsequent dynamic full cure cycles (5 K min^{-1}, right).

Table 1
TGA data for B-staging and C-staging of catalyzed PFA resin. Dynamic temperature profiles and heating between isothermal plateaus were performed at 5 K min^{-1}.

A-stage to B-stage (B-staging)				B-stage to C-stage (Full cure)			
Cure cycle	Max. rate[wt% min^{-1}]	Temperature at max. rate [°C]	Weight loss [wt %]	Cure cycle	Max. rate [wt% min^{-1}]	Temperature at max. rate [°C]	Weight loss [wt %]
50 °C, 2 h	0.309 ± 0.065	50.2	8.18 ± 0.35	20 to 300 °C, 5 K min^{-1}	0.466 ± 0.035	142.6	17.67 ± 0.36
60 °C, 2 h	0.438 ± 0.042	60.4	9.48 ± 0.72	20 to 300 °C, 5 K min^{-1}	0.380 ± 0.032	144.5	17.72 ± 0.72
70 °C, 2 h	0.581 ± 0.099	70.5	10.40 ± 1.02	20 to 300 °C, 5 K min^{-1}	0.351 ± 0.044	144.5	17.97 ± 0.74
80 °C, 2 h	0.557 ± 0.079	80.6	11.41 ± 0.80	20 to 300 °C, 5 K min^{-1}	0.249 ± 0.057	144.6	18.13 ± 0.90
90 °C, 2 h	0.568 ± 0.123	90.6	12.94 ± 1.34	20 to 300 °C, 5 K min^{-1}	0.177 ± 0.041	150.5	18.31 ± 0.64
–	–	–	–	90, 120, 150 °C á 30 min	0.683 ± 0.126	90.4	15.58 ± 0.44
60 °C, 2 h	0.443 ± 0.051	60.5	9.88 ± 0.84	90, 120, 150 °C á 30 min	0.110 ± 0.029	120.2	16.02 ± 0.48

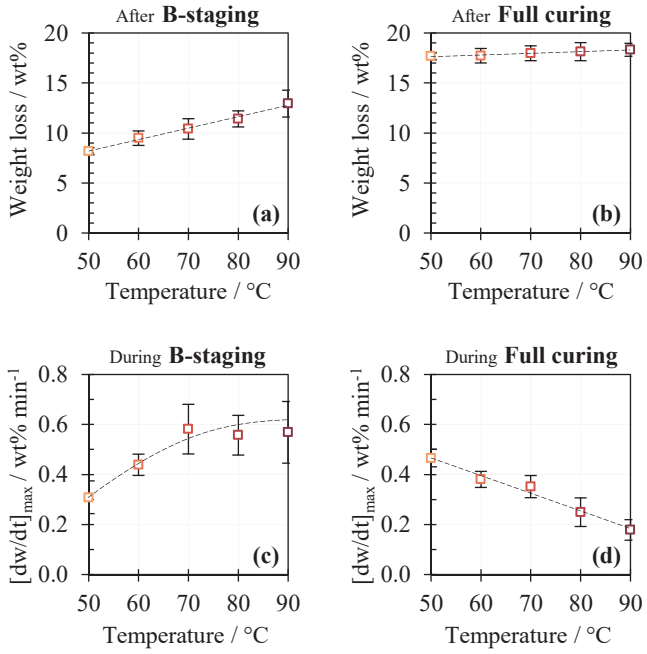

Fig. 9. Weight loss (a, c) and maximum weight loss rate (b, d) as a function of B-staging temperature after pre-cure (B-stage, left) and full cure (C-stage, right).

Table 2
Pre-cure degrees (DoC) of PFA resins after variable temperature B-staging procedures calculated from DSC data. DSC enthalpies were used relative to the initial sample weight (left) and adjusted to the TGA weight loss (right).

B-staging	Constant sample weight		Weight-adjusted by TGA	
	Enthalpy [J g^{-1}]	DoC [%]	Enthalpy [J g^{-1}]	DoC [%]
Fresh	130.0	0	143.6	0
50 °C	113.7	12.5	130.6	9.1
60 °C	84.1	35.3	97.3	32.2
70 °C	69.6	46.5	81.1	43.5
80 °C	61.5	52.7	72.1	49.7
90 °C	34.2	73.7	40.5	71.8

prepolymerization and/or in the methodology of analyzing the DSC data. Odiyi et al. [37] measured 273 J g^{-1} for commercial PFA prepregs when being exposed to a dynamic temperature profile of 5 K min. In another study [38], very high exothermic enthalpies for isothermal curing of up to 700 J g^{-1} were reported that can be explained as follows: Sealed pans were used to eliminate endothermic volatile evaporation and, particularly, PFA was polymerized and cured in-situ from FA and acid instead of synthesizing a prepolymer beforehand. From this insight, it could be deduced that the greater part of the exothermic reaction was already taking place during prepolymer synthesis.

As the present study is the first in literature to examine B-staging of PFA, there was only data from the petrochemical pendant of PFA, phenolic resin, to compare to. Gupta et al. [39] found the residual heat of B-staged phenolic resin to be as low as 35.2 J g^{-1}. Szpoganicz et al. [34] reported a DSC exothermic enthalpy of 96 J g^{-1} corresponding to a pre-curing of 36 % which was close to the PFA values at 97.3 J g^{-1} and 32.2 %.

As expected due to the mass loss, the weight-adjusted enthalpies of Table 2 were consistently higher than the original DSC enthalpies which were determined for a constant initial sample weight. The adjusted degree of pre-cure from B-staging was found to be 2–3 % lower. The following results relate to the TGA-adjusted DSC data. 0 % DoC relate to the catalyzed A-stage PFA resin right after prepolymerization. Comparing the rheological data of B-staged PFA to a commercial epoxy-based prepreg resin had already revealed that after 2 h of B-staging at 60 °C, similar temperature-dependent viscosities and storage moduli could be observed. According to Table 2, the corresponding degree of pre-cure amounted to 32.2 % for PFA. This value ranked in the middle of the range proposed as optimal for phenolic prepregs in terms of tack and flow properties [40]. It was also in accordance with findings for epoxy-based prepregs of 30 % DoC, which in this condition allowed the prepreg to be deformed during lay-up, exhibits little residual stress after shearing and has high adhesive tack strength with a metallic tool surface [41].

The curing progress, as explored by DSC, was also evident in the evaluation of the GPC chromatograms presented in Fig. 10. Here, the refractive index as the detector response was plotted as a function of retention time. The data were not calibrated against polystyrene as different hydrodynamic behavior per molecular weight was expected due to fundamental differences in the molecular structure (linear vs. branched and cross-linked). Nevertheless, a significant shift towards higher hydrodynamic volume could be observed as B-staging progressed. At the same time, the initially large peaks at high retention volumes (monomer and oligomer fractions) progressively decreased indicating cure progression by linear chain growth and cross-linking. Peak expansion was observed that was representative of a broad size distribution in the B-stage, particularly in the highly pre-cured samples. Analyzing the PFA prepolymer and catalyzed but not pre-cured A-stage resin (0 min) resulted in close to identical curves. It can therefore be concluded that pTSA catalysis apparently did not immediately trigger curing at room temperature which is to be regarded positive in terms of room temperature storability for prepreg applications.

In an effort to explore the changes in the molecular fingerprint, FTIR

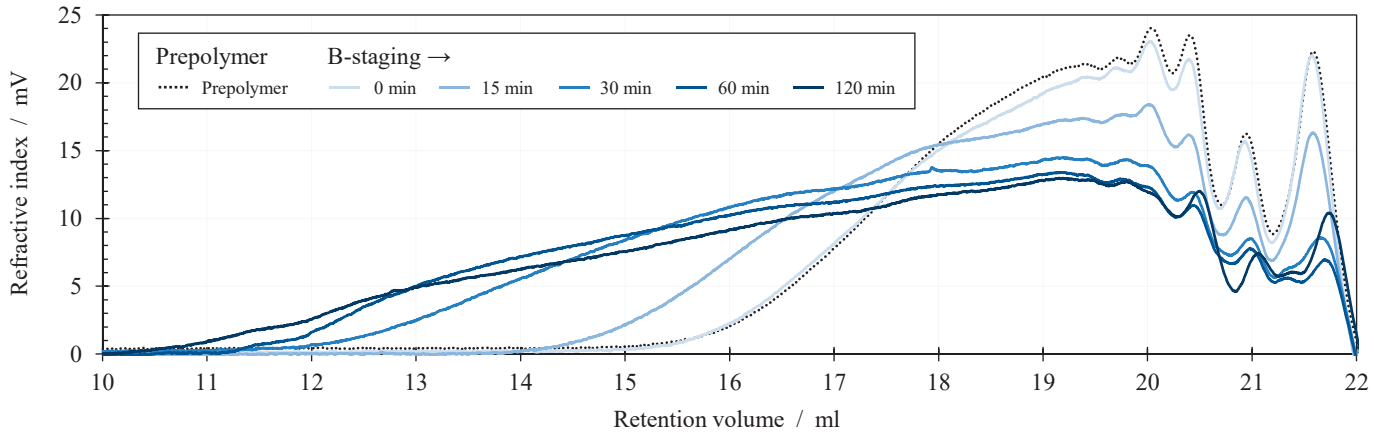

Fig. 10. GPC chromatograms of PFA prepolymer and resins B-staged at 60 °C for different time spans.

spectroscopy was employed on catalyzed resin samples throughout the 60 °C B-staging procedure. Fig. 11 shows the absorbance spectra in the mid-infrared range between 500 and 4000 cm^{-1}. The spectra were in good agreement with those from previous FTIR studies on PFA polymerization [18,36,42] as most recorded absorption bands could be attributed to the characteristic molecular vibrations. Within the FTIR high-wavenumber region of 3200–3600 cm^{-1}, the influence of increasing B-staging times did not result in a clear trend with respect to the presence of void-inducing water. Reasons are that there are at least three contributors affecting this region, namely residual alcohol O-H from furfuryl alcohol, hydrogen-bonded hydroxyl groups in partially reacted polymer, and water. During polymerization, O-H groups of FA and partially reacted PFA were constantly consumed while water was produced – two mechanisms which contributed to the formation of the broad peak in opposite ways. However, the highest absorbance was recorded for 120-min B-staged PFA (dark blue line) indicating the highest amount of unevaporated water and an incomplete thermosetting process. This peak is not expected to be present any longer in the spectrum of fully cured PFA.

Moving to lower wavenumbers, two distinct peaks began to form following long pre-curing at 2850 and 2920 cm^{-1} representing the symmetric and asymmetric aliphatic methylene bridges between furan rings and are, therefore, indicative of crosslinking. A substantial increase relative to the initial monomer spectrum was recorded for B-staging times of 60 and 120 min, respectively. Another indicator crosslinking progress was the broadening of the aromatic C=C band region (1510–1560 cm^{-1}), resulting from increased disorder and conjugation. The intensification of the peak at 1560 cm^{-1} as part of 2,5-disubstituted furan rings also suggested the progressing development of the polymeric network. A further distinctive peak, which increased as a function of B-staging time, could be observed at 1715 cm^{-1} at the carbonyl (C=O) stretching vibration that is not intrinsically contained in FA. Its presence indicated ring opening under highly acidic conditions, though it may also have been affected by oxidative degradation. The fact that this peak was already observed in the A-stage resin (0 min) is evidence to suggest that at a certain degree of network was already present in the prepolymer state.

General difficulties arose when attempting to make precise mechanistic claims in the fingerprint region due to the complexity of molecular vibrations. E.g., the loss of alcohol functionality, which represents monomer consumption in the region around 1012 cm^{-1}, (C-O stretch of $–CH_2OH$) was not significant contrary to expectations. Either the proportion of unreacted FA was similarly low in all samples, or the results were influenced by measurement distortions related to normalization, ATR contact pressure sensitivity, surface composition, or penetration depth.

4.3. *Isothermally full-cured resins (C-stage)*

Industry-standard curing cycles for composite manufacturing from prepregs typically include two or more consecutive isothermal steps to control excessive exothermic reactions and/or potential resin bleed. Therefore, a curing cycle between 90 °C and 150 °C was proposed featuring stepwise temperature increases of 30 °C and dwell times of 30 min. It was applied to the processing-optimized B-stage resin pre-cured at 60 °C and to the catalyzed A-stage resin (reference).

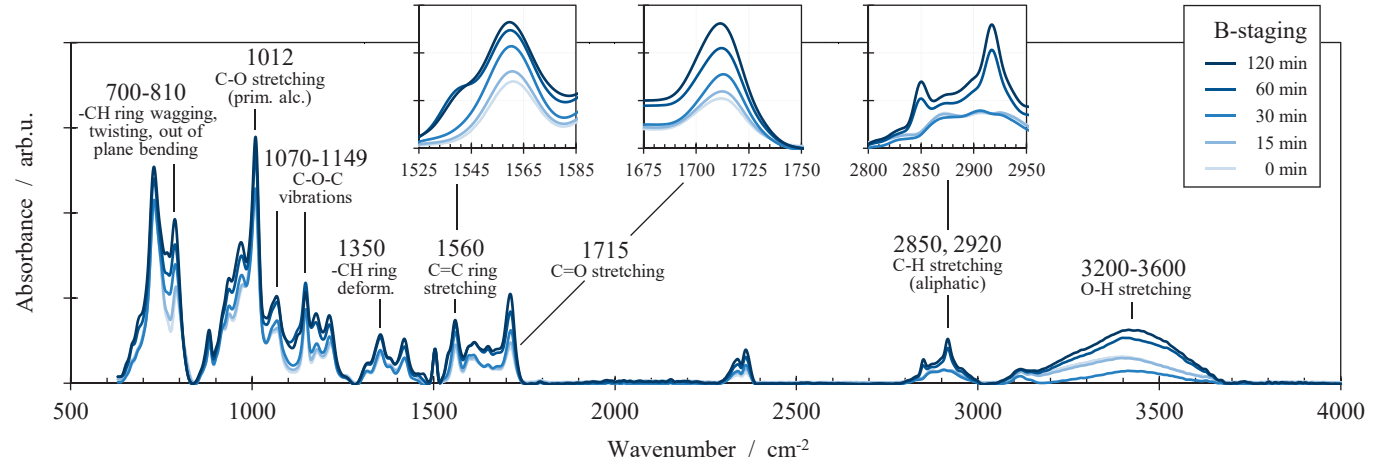

Fig. 11. FTIR spectra of PFA resins B-staged at 60 °C for different time spans.

4.3.1. Impact of preceding B-staging

In Fig. 12, a comparison between fresh (black) and B-staged (60 °C, orange) PFA resin was drawn in terms of volatile weight loss during the step-wise curing cycle outlined above. The corresponding numerical data is given in the last two rows of Table 1. With regard to the impact of preceding B-staging, both weight loss curves disproportionately trended downwards when entering the curing cycle at the 120-minute mark. Fresh PFA quickly started releasing a significant quantity of volatiles as soon reaching 90 °C with a peak loss rate close to 0.7 wt% min^{-1}. Both the maximum loss rates and lost weight fractions were more than halved for each consecutive temperature step. Meanwhile, the pre-cured PFA lost ~ 10 wt% during B-staging – the same quantity of volatiles as fresh resin during the first curing step but at a significantly slower rate. The consecutive curing steps only involved weight losses of a few percent and maximum loss rates of 0.1 wt% min^{-1}.

Ultimately, isothermal curing at temperatures up to 150 °C resulted in a C-stage resin that suffered a total weight loss of 15.58 and 16.02 wt %, respectively. These values were approximately 2 wt% lower than for resins that were cured dynamically up to 300 °C. The small difference in weight loss was attributed to residual unreacted FA which generally evaporates at temperatures as high as 170 °C. Also, the time and temperature dependent diffusion rate of other volatiles such as water could also have contributed to the difference. Notwithstanding, the drop in loss rate to virtually zero indicated a practically fully cured resin after 30 min at 150 °C. It was therefore assumed that the proposed curing cycle was suitable for the manufacture of composite components. The fact that a considerable quantity of volatiles was already discarded throughout B-staging, porosity through void formation was expected to decrease as a function of pre-curing. The hypothesis will be tested in the following.

4.3.2. Porosity

The porosity of resin samples that had been B-staged and fully cured was monitored via light microscopy of polished cross-sections. Porosity evaluation through microscopy is known to be section-biased [43], which means results may depend on the selection and direction of the two-dimensional area of interest. Here, the section bias effect was eliminated in radial direction by analyzing the whole sample cross-section. However, it remained in axial direction of the cylindrical specimen. Density measurement is a more global analysis method, albeit one that is unable to differentiate locally. In an effort to gain first insights into global porosity, the densities of cured PFA resins were assessed by Archimedes' method as shown in Fig. 13.

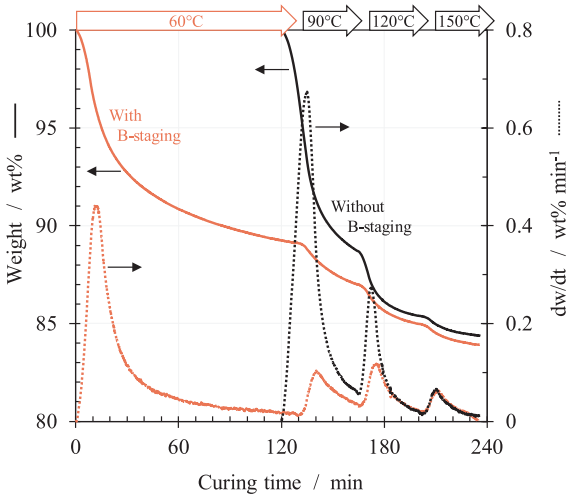

Fig. 12. Comparison of volatile separation between B-staged and A-stage PFA resins during an isothermal curing profile with consecutive 30-minute dwells at 90, 120 and 150 °C.

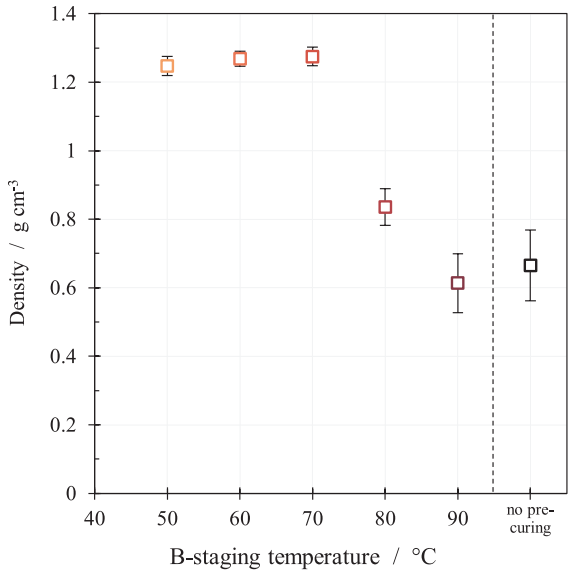

Fig. 13. C-stage PFA resin densities determined via Archimedes' principle.

The densities of low-temperature pre-cured samples were found to be between 1.24 and 1.28 g cm^{-3}. which was lower than the initial 1.4 g cm^{-3} measured for A-stage resin in this study and reported elsewhere [44]. The difference of ~ 10 wt% was significantly smaller than the volatile weight loss measured by TGA. Consequently, a certain residual porosity of few percent was expected to be present in these samples. For higher B-staging temperatures, a considerable decrease of density was observed which was indicative of massive void formation and entrapment within the resin. Samples without preceding pre-curing showed the same level of density as samples that were pre-cured at 90 °C. On the one hand, this outcome was expected because the initial dwell temperature matched the B-staging temperature of 90 °C. On the other hand, the result showed that the process of void formation was fully completed within the first 30 min at 90 °C with no further influence of the subsequent dwell stages at 120 and 150 °C, respectively.

In an effort to characterize void formation in PFA in detail, micrographs of polished resin samples were assessed following the analysis procedure described in section 3.6. The results of porosity measurement in combination with representative surface images are presented in Fig. 14. In accordance with the density results of Fig. 13, low and medium B-staging temperatures reproducibly led to low porosities of 2.5 (50 °C), 3.2 (60 °C), and 4.3 % (70 °C). This level of porosity was characterized by a large number of micropores that were distributed evenly through the resin sample in both radial and z-direction. An average of more than 29,000 micropores were detected in the cross-sections of 60 °C samples that measured a total area of 254 mm^2. The minimum detectable pore size was 37 μm^2 and the average pore size was 215 μm^2 with a very similar pore structure found in 50 °C samples. The slightly increased overall porosity observed for 70 °C samples were due to an increased average pore size (452 μm^2) despite a lower average amount of pores (18.000).

The corresponding pore size distributions are displayed in Fig. 15. Few but large voids in the 70 °C samples shifted the cumulated relative porosity towards the right-hand side of the pore size spectrum. Meanwhile, the graphs of 50 and 60 °C PFA samples showed similar trends and did not exceed a pore size of 10^4 μm^2 equaling a diameter of ~ 35 μm.

The exclusive presence of micropores suggested that during B-staging between 50 and 70 °C, the water from polycondensation did not evaporate before resin gelation. Therefore, micropores neither expanded nor migrated at ambient pressure so that the micropores remained in place before the resin gelled. The subsequent temperature elevation to

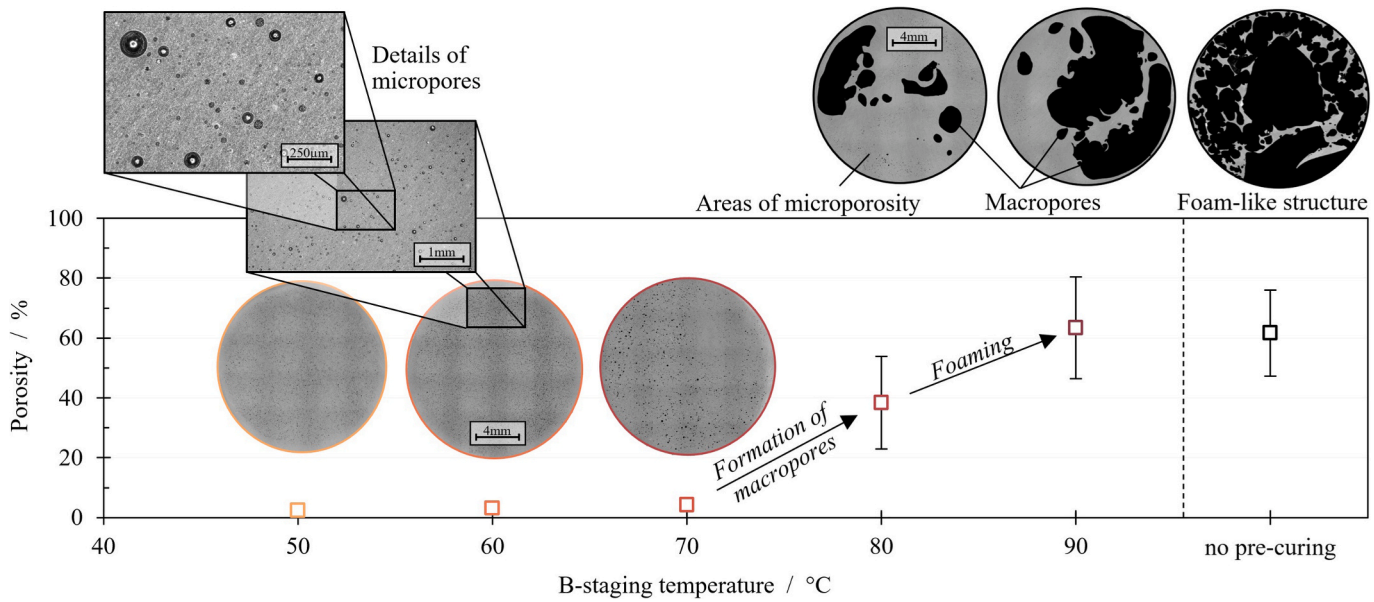

Fig. 14. Influence of B-staging on the porosity (black) of fully cured PFA resins. Micrographs of macropores and foaming are representative of all samples which were B-staged at 80 and 90 °C or cured directly.

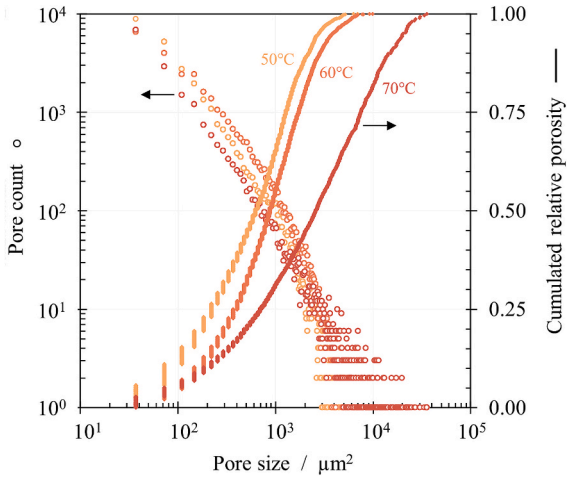

Fig. 15. Pore size distributions of microporous, cured PFA samples with preceding B-staging at 50, 60 and 70 °C.

90, 120 and 150 °C apparently did not influence the pore structure during the final curing cycle. The observed formation of micropores during low-temperature B-staging was attributed to the continuous polymerization-induced formation of water which at some point would no longer be soluble in the PFA resin. Pores of liquid water formed as soon as the limit of the resin's temperature-dependent water solubility was reached. As the B-staging temperature was well below the ambient pressure evaporation temperature of the involved liquids, i.e., mainly water (100 °C), unreacted furfuryl alcohol (170 °C) and a mixture of both (92 °C), micropores did not expand significantly due to boiling.

A different resin morphology developed for cured samples that were either B-staged at 80/90 °C or were directly subjected to the final curing cycle. The corresponding cross-sections shown on the right-hand side of Fig. 14 display massive formation of macroscopic voids which measured several square millimeters. The macropores started to form at a B-staging temperature of 80 °C resulting in an average porosity of 38.3 %. Pre-curing at 90 °C raised the porosity to a total level of 63.3 % while no further increase was observed if the resins were cured directly. Here, foam-like structures were formed which locally reached porosities of more than 80 %. Accordingly, the standard deviations of ~ 15 % were rather high due to different resin morphologies throughout the sample: While the foam-like structures could be observed especially in the surface-near top layers of the resin samples, denser regions were found towards the bottom. Areas around the macropores still exhibited a certain degree of microporosity. In a different study focusing on the influences of initial resin viscosity, moisture and pH on void formation in cured PFA, porosities between 5.58 and 43.26 % in combination with average pore sizes between 9.47 and 194.30 µm were reported [45]. The DoE revealed the most crucial effects originating from moisture, followed by the adjustment of pH by resin neutralization. Here, the aim was the rigid control of the processing parameters for obtaining monolithic vitreous carbon (MVC) rather than tailoring PFA resins for prepreg applications.

According to the well-understood void formation and growth theory for composites [46–48], the transition of pores from micro to macro scale in homogenous media (without reinforcement fibers) takes place as soon as the void pressure exceeds the hydrostatic pressure in the surrounding resin. The liquid/vapor phase transition is linked to a massive volume increase that is triggered by volatile boiling. Although the boiling temperatures were not reached by the nominal temperatures of 80 and 90 °C, respectively, exothermicity of the rapidly proceeding reaction may have led to temporary overheating and, thus, void growth. Higher temperatures generally lead to faster water diffusion through thermoset resins. Water from surrounding areas accumulated in pores quicker and favored the formation of larger pores. Furthermore, the quick viscosity increase and resin gelation at high temperatures prevented volatile bubbles from rising through the PFA and eventually collapsing at the resin surface.

5. Conclusion and future perspectives

In this study, a thermoset bio-resin based on acid-catalyzed furfuryl alcohol was synthesized and characterized for prepreg applications at different stages of processing. Special emphasis was put on the B-stage that serves as a processing-optimized intermediate state between the initial post-synthesis (A-stage) and the fully cured (C-stage) state. Different isothermal B-staging procedures were applied in an effort to examine their effects on rheology, reactivity, volatile release and part porosity. The main findings can be summarized as follows:

- A short curing cycle of 142 min (30 min consecutive dwells at 90, 120 and 150 °C) including heating and cooling ramps was demonstrated to produce fully cured PFA.
- Up to 18.3 wt% of the sample were split off during cure in the form of volatiles, i.e., mainly water and unreacted FA.
- Direct curing of A-stage PFA resins led to the formation of macro pores and a low-density, foam-like structure.
- By pre-curing to a B-stage, more than 50 % of the total volatiles could be eliminated prematurely and were no longer be present in the resin to form voids upon final cure.
- The combination of TGA and DSC revealed a substantial decrease in resin reactivity upon final cure if the PFA had been B-staged beforehand.
- As a consequence, part porosity could be reduced from a reference value of 61.7 % to less than 3 % accompanied by full oppression of macro voids.
- 120 min of isothermal B-staging at 60 °C resulted in rheological characteristics that matched the data of commercial epoxy prepregs and, hence, promised favorable processing properties such as tack and drape.
- The degree of pre-cure after this B-staging procedure was found to be 32.2 % in relation to the A-stage. On the way there, the molecular weight increased as a function of B-staging duration due to accretive chain growth and network formation as monitored by FTIR.

The findings illustrate the obstacles of making acid-catalyzed PFA resins industrially viable for bio-based composite applications. Porosity as a result of volatiles produced from polycondensation remains a challenge that was demonstrated to be approachable through informed B-staging of the resin. Based on the results of this study, it is recommended that a 120-minute pre-curing procedure at 60 °C be implemented to improve both the processing properties of prepregs and the quality of the resulting parts. However, both aspects will have to be verified in future research as the study was limited to neat resin at atmospheric pressure. With a view to transition the resin-based findings towards prepregs and composite components, several questions are yet to be answered. It specifically remains to be proven that the void mitigation strategy by pre-curing is applicable to the conditions of composites manufacturing. Here, the influences of consolidation pressure, fiber reinforcement and laminate stacking sequence on void formation, growth and suppression are of great interest. Furthermore, PFA prepregs will be produced and characterized in terms of their processing properties. The temperature-dependency of processing properties including drape and tack is crucial to enable informed process adjustment, e.g., for automated fiber placement (AFP) or other prepreg-based processing routes. The thermo-mechanical performance of both fully cured neat resin and composites will be investigated for different PFA formulations and fiber–matrix combinations at varying manufacturing cycles. In particular, material characteristics such as stiffness, strength and fracture toughness are expected to be influenced not only by voids, but also by the formation and constitution of the polymer network.

CRediT authorship contribution statement

Dennis Budelmann: Writing – review & editing, Writing – original draft, Visualization, Methodology, Investigation, Funding acquisition, Formal analysis, Data curation, Conceptualization. **Bodo Fiedler:** Writing – review & editing, Resources, Project administration.

Declaration of competing interest

The authors declare that they have no known competing financial interests or personal relationships that could have appeared to influence the work reported in this paper.

Acknowledgements

The authors are grateful for the financial support by Deutsche Forschungsgemeinschaft (DFG – German Research Foundation) granted for the research project 'FurPreg' (project number 559990233). Gratitude is expressed to Dr. Sarah-Franziska Stahl and Angelina Aran Pinnschmidt (Schill + Seilacher "Struktol" GmbH) for organizing and conducting the GPC experiments.

Data availability

Data will be made available on request.

References

[1] M. Derradji, O. Mehelli, W. Liu, N. Fantuzzi, Sustainable and Ecofriendly Chemical Design of High Performance Bio-Based Thermosets for Advanced applications, Front. Chem. 9 (2021) 691117, https://doi.org/10.3389/fchem.2021.691117.
[2] J. Liu, L. Zhang, W. Shun, J. Dai, Y. Peng, X. Liu, Recent development on bio-based thermosetting resins, J. Polym. Sci. 59 (2021) 1474–1490, https://doi.org/10.1002/pol.20210328.
[3] A. Gomez-Campos, C. Vialle, A. Rouilly, L. Hamelin, A. Rogeon, D. Hardy, et al., Natural Fibre Polymer Composites - a game changer for the aviation sector? J. Clean. Prod. 286 (2021) 124986 https://doi.org/10.1016/j.jclepro.2020.124986.
[4] P. Roy, F. Defersha, A. Rodriguez-Uribe, M. Misra, A.K. Mohanty, Evaluation of the life cycle of an automotive component produced from biocomposite, J. Clean. Prod. 273 (2020) 123051, https://doi.org/10.1016/j.jclepro.2020.123051.
[5] A. Lopez-Arraiza, L. Essamari, M. Iturrondobeitia, D. Boullosa-Falces, D. Justel, Life cycle assessment of glass fibre versus flax fibre reinforced composite ship hulls, Sci. Rep. 15 (2025) 16283, https://doi.org/10.1038/s41598-025-00811-y.
[6] U. Kirschnick, B. Ravindran, M. Sieberer, E. Fauster, M. Feuchter, The Fossil, the Green, and the In-between: Life Cycle Assessment of Manufacturing Composites with Varying Bio-based Content, J Compos Sci 9 (2025) 93, https://doi.org/10.3390/jcs9030093.
[7] S.K. Bardhan, S. Gupta, M.E. Gorman, M.A. Haider, Biorenewable chemicals: Feedstocks, technologies and the conflict with food production, Renew. Sustain. Energy Rev. 51 (2015) 506–520, https://doi.org/10.1016/j.rser.2015.06.013.
[8] Z. An, J. Li, Recent advances in the catalytic transfer hydrogenation of furfural to furfuryl alcohol over heterogeneous catalysts, Green Chem. 24 (2022) 1780–1808, https://doi.org/10.1039/D1GC04440K.
[9] A.P. Dunlop, F.N. Peters, The Nature of Furfuryl Alcohol, Ind. Eng. Chem. 34 (1942) 814–817, https://doi.org/10.1021/ie50391a010.
[10] Gandini A. The behaviour of furan derivatives in polymerization reactions. Polym. Chem., vol. 25, Berlin, Heidelberg: Springer Berlin Heidelberg; 1977, p. 47-96. doi: 10.1007/3-540-08389-8_6.
[11] A.O.C. Iroegbu, S.S. Ray, On the chemistry of furfuryl alcohol polymerization: a review, J. Polym. Sci. 62 (2024) 1044–1060, https://doi.org/10.1002/pol.20230708.
[12] S.D. Oguntuyi, K. Nyembwe, M.B. Shongwe, T. Mojisola, Challenges and recent progress on the application of rapid sand casting for part production: a review, Int. J. Adv. Manuf. Technol. 126 (2023) 891–906, https://doi.org/10.1007/s00170-023-11049-1.
[13] X. Shen, S. Yang, G. Li, S. Liu, F. Chu, The contribution mechanism of furfuryl alcohol treatment on the dimensional stability of plantation wood, Ind. Crops Prod. 186 (2022) 115143, https://doi.org/10.1016/j.indcrop.2022.115143.
[14] I. Ekop, I.-I.-N. Etim, E. Ambrose, U.E. Edike, Bio-based Cement Concrete Admixtures for Green Recovery in the Construction Industry: a critical Survey, Mater. Circ. Econ. 6 (2024) 31, https://doi.org/10.1007/s42824-024-00113-0.
[15] U. Lopez De Vergara, M. Sarrionandia, K. Gondra, J. Aurrekoetxea, Polymerization and curing kinetics of furan resins under conventional and microwave heating, Thermochim Acta 581 (2014) 92–99, https://doi.org/10.1016/j.tca.2014.02.017.
[16] J.C. Domínguez, J.C. Grivel, B. Madsen, Study on the non-isothermal curing kinetics of a polyfurfuryl alcohol bioresin by DSC using different amounts of catalyst, Thermochim Acta 529 (2012) 29–35, https://doi.org/10.1016/j.tca.2011.11.018.
[17] J.C. Domínguez, B. Madsen, Chemorheological study of a polyfurfuryl alcohol resin system—Pre-gel curing stage, Ind. Crops Prod. 52 (2014) 321–328, https://doi.org/10.1016/j.indcrop.2013.11.006.
[18] F. D'Amico, M.E. Musso, R.J.F. Berger, N. Cefarin, G. Birarda, G. Tondi, et al., Chemical constitution of polyfurfuryl alcohol investigated by FTIR and Resonant Raman spectroscopy, Spectrochim. Acta A Mol. Biomol. Spectrosc. 262 (2021) 120090, https://doi.org/10.1016/j.saa.2021.120090.
[19] A. Minini, F. Becagli, J. Nieri, S. Armillei, C. Mingazzini, Mechanical Characterizations on biobased Sheet Molding compound (SMC) developed for battery boxes, J. Phys. Conf. Ser. 2692 (2024) 012011, https://doi.org/10.1088/1742-6596/2692/1/012011.
[20] U. López De Vergara, M. Sarrionandia, K. Gondra, J. Aurrekoetxea, Impact behaviour of basalt fibre reinforced furan composites cured under microwave and thermal conditions, Compos. Part B Eng. 66 (2014) 156–161, https://doi.org/10.1016/j.compositesb.2014.05.009.

[21] D. Budelmann, D. Gibhardt, B. Fiedler, A review on aging effects of thermoset prepregs, Compos. Part B Eng. 303 (2025) 112611, https://doi.org/10.1016/j.compositesb.2025.112611.
[22] R. Crossley, P. Schubel, A. Stevenson, Furan matrix and flax fibre as a sustainable renewable composite: Mechanical and fire-resistant properties in comparison to phenol, epoxy and polyester, J. Reinf. Plast. Compos. 33 (2014) 58–68, https://doi.org/10.1177/0731684413502108.
[23] P. Ares Elejoste, A. Allue, J. Ballestero, S. Neira, J.L. Gómez-Alonso, K. Gondra, Development and Characterisation of Sustainable Prepregs with improved Fire Behaviour based on Furan Resin and Basalt Fibre Reinforcement, Polymers 14 (2022) 1864, https://doi.org/10.3390/polym14091864.
[24] M. Foruzanmehr, S. Elkoun, A. Fam, M. Robert, Degradation characteristics of new bio-resin based-fiber-reinforced polymers for external rehabilitation of structures, J. Compos. Mater. 50 (2016) 1227–1239, https://doi.org/10.1177/0021998315590262.
[25] D.C. Odiyi, T. Sharif, R.S. Choudhry, S. Mallik, S.Z.H. Shah, A review of advancements in synthesis, manufacturing and properties of environment friendly biobased Polyfurfuryl Alcohol Resin and its Composites, Compos. Part B Eng. 267 (2023) 111034, https://doi.org/10.1016/j.compositesb.2023.111034.
[26] J. Domínguez, B. Madsen, Development of new biomass-based furan/glass composites manufactured by the double-vacuum-bag technique, J. Compos. Mater. 49 (2015) 2993–3003, https://doi.org/10.1177/0021998314559060.
[27] K. Resch-Fauster, J. Džalto, A. Anusic, P. Mitschang, Effect of the water absorptive capacity of reinforcing fibers on the process ability, morphology, and performance characteristics of composites produced from polyfurfuryl alcohol, Adv. Manuf. Polym. Compos. Sci. 4 (2018) 1323, https://doi.org/10.1080/20550340.2018.1436234.
[28] C. Pupin, A. Ross, C. Dubois, J.-C. Rietsch, E. Ruiz, Predicting porosity formation in phenolic resins for RTM manufacturing: the porosity map, Compos Part Appl Sci Manuf 100 (2017) 294–304, https://doi.org/10.1016/j.compositesa.2017.05.023.
[29] E.M. Wewerka, E.D. Loughran, K.L. Walters, A study of the low molecular weight components of furfuryl alcohol polymers, J. Appl. Polym. Sci. 15 (1971) 1437–1451, https://doi.org/10.1002/app.1971.070150612.
[30] R. Marefat Seyedlar, M. Imani, S.M. Mirabedini, Rheokinetics in curing process of polyfurfuryl alcohol: effect of homologous acid catalysts, Iran. Polym. J. 26 (2017) 281–293, https://doi.org/10.1007/s13726-017-0518-0.
[31] D. Budelmann, C. Schmidt, D. Meiners, Adhesion-cohesion balance of prepreg tack in thermoset automated fiber placement. Part 1: Adhesion and surface wetting. Compos Part C Open, Access 6 (2021) 100204, https://doi.org/10.1016/j.jcomc.2021.100204.
[32] A. Endruweit, G.Y.H. Choong, S. Ghose, B.A. Johnson, D.R. Younkin, N.A. Warrior, et al., Characterisation of tack for uni-directional prepreg tape employing a continuous application-and-peel test method, Compos Part Appl Sci Manuf 114 (2018) 295–306, https://doi.org/10.1016/j.compositesa.2018.08.027.
[33] J. Shi, W. Wang, Y. Wang, J. Qi, J. Xiao, A Peel Test Method to Characterize the Decay Law of Prepreg Tape tack at Different Temperatures, Materials 17 (2024) 2449, https://doi.org/10.3390/ma17102449.
[34] E. Szpoganicz, M. Demleitner, F. Hübner, Y. Oh, Y. Kweon, H. Lee, et al., Phenolic prepregs for automated composites manufacturing – Correlation of rheological properties and environmental factors with prepreg tack, Compos. Sci. Technol. 218 (2022) 109188, https://doi.org/10.1016/j.compscitech.2021.109188.
[35] N. Guigo, A. Mija, R. Zavaglia, L. Vincent, N. Sbirrazzuoli, New insights on the thermal degradation pathways of neat poly(furfuryl alcohol) and poly(furfuryl alcohol)/SiO2 hybrid materials, Polym. Degrad. Stab. 94 (2009) 908–913, https://doi.org/10.1016/j.polymdegradstab.2009.03.008.
[36] G. Tondi, N. Cefarin, T. Sepperer, F. D'Amico, R.J.F. Berger, M. Musso, et al., Understanding the Polymerization of Polyfurfuryl Alcohol: Ring opening and Diels-Alder Reactions, Polymers 11 (2019) 2126, https://doi.org/10.3390/polym11122126.
[37] D.C. Odiyi, T. Sharif, R.S. Choudhry, S. Mallik, Cure mechanism and kinetic prediction of biobased glass/polyfurfuryl alcohol prepreg by model-free kinetics, Thermochim Acta 708 (2022) 179133, https://doi.org/10.1016/j.tca.2021.179133.
[38] N. Guigo, A. Mija, L. Vincent, N. Sbirrazzuoli, Chemorheological analysis and model-free kinetics of acid catalysed furfuryl alcohol polymerization, Phys. Chem. Chem. Phys. 9 (2007) 5359, https://doi.org/10.1039/b707950h.
[39] N. Gupta, A.R. Mahendran, S. Weiss, M. Khalifa, Thermal curing behavior of phenol formaldehyde resin-impregnated paper evaluated using DSC and dielectric analysis, J. Therm. Anal. Calorim. 149 (2024) 2609–2618, https://doi.org/10.1007/s10973-023-12843-5.
[40] M. Rajaei, M.H. Beheshty, M. Hayaty, Preparation and Processing Characterization of Glass/Phenolic Prepregs, Polym. Polym. Compos. 19 (2011) 789–796, https://doi.org/10.1177/096739111101900909.
[41] R. Banks, A.P. Mouritz, S. John, F. Coman, R. Paton, Development of a new structural prepreg: characterisation of handling, drape and tack properties, Compos. Struct. 66 (2004) 169–174, https://doi.org/10.1016/j.compstruct.2004.04.034.
[42] E.A. Psochia, P. Delliere, R. Sanchez, K.S. Triantafyllidis, N. Guigo, Sustainable alliance between nanocellulose and biobased polyfurfuryl alcohol, Ind. Crops Prod. 212 (2024) 118346, https://doi.org/10.1016/j.indcrop.2024.118346.
[43] Y.K. Hamidi, L. Aktas, M.C. Altan, Three-dimensional features of void morphology in resin transfer molded composites, Compos. Sci. Technol. 65 (2005) 1306–1320, https://doi.org/10.1016/j.compscitech.2005.01.001.
[44] C. Menager, N. Guigo, X. Wu, L. Vincent, N. Sbirrazzuoli, "Green" composites prepared from polyfurfuryl alcohol and cork residues: thermal and mechanical properties, Compos Part Appl Sci Manuf 124 (2019) 105473, https://doi.org/10.1016/j.compositesa.2019.105473.
[45] S.S. Oishi, M.C. Rezende, F.D. Origo, A.J. Damiao, E.C. Botelho, Viscosity, pH, and moisture effect in the porosity of poly(furfuryl alcohol), J. Appl. Polym. Sci. 128 (2013) 1680–1686, https://doi.org/10.1002/app.38332.
[46] C.H. Park, L. Woo, Modeling void formation and unsaturated flow in liquid composite molding processes: a survey and review, J. Reinf. Plast. Compos. 30 (2011) 957–977, https://doi.org/10.1177/0731684411411338.
[47] L.K. Grunenfelder, S.R. Nutt, Void formation in composite prepregs – effect of dissolved moisture, Compos. Sci. Technol. 70 (2010) 2304–2309, https://doi.org/10.1016/j.compscitech.2010.09.009.
[48] M. Mehdikhani, L. Gorbatikh, I. Verpoest, S.V. Lomov, Voids in fiber-reinforced polymer composites: a review on their formation, characteristics, and effects on mechanical performance, J. Compos. Mater. 53 (2019) 1579–1669, https://doi.org/10.1177/0021998318772152.